

# Properties of nitrogen doped silicon films deposited by low-pressure chemical vapor deposition from silane and ammonia

P. Temple-Boyer,<sup>a)</sup> L. Jalabert, and L. Masarotto  
LAAS-CNRS, 7 Avenue du Colonel Roche, 31077 Toulouse Cedex 4, France

J. L. Alay and J. R. Morante  
Departamento d'Electronica, Facultat de Fisica, Universitat de Barcelona, Av. Diagonal 645,  
08028 Barcelona, Spain

(Received 28 October 1999; accepted 12 May 2000)

Nitrogen doped silicon (NIDOS) films have been deposited by low-pressure chemical vapor deposition from silane  $\text{SiH}_4$  and ammonia  $\text{NH}_3$  at high temperature ( $750^\circ\text{C}$ ) and the influences of the  $\text{NH}_3/\text{SiH}_4$  gas ratio on the films deposition rate, refractive index, stoichiometry, microstructure, electrical conductivity, and thermomechanical stress are studied. The chemical species derived from silylene  $\text{SiH}_2$  into the gaseous phase are shown to be responsible for the deposition of NIDOS and/or (silicon rich) silicon nitride. The competition between these two deposition phenomena leads finally to very high deposition rates ( $\approx 100$  nm/min) for low  $\text{NH}_3/\text{SiH}_4$  gas ratio ( $R \approx 0.1$ ). Moreover, complex variations of NIDOS film properties are evidenced and related to the dual behavior of the nitrogen atom into silicon, either *n*-type substitutional impurity or insulative interstitial impurity, according to the Si–N atomic bond. Finally, the use of NIDOS deposition for the realization of microelectromechanical systems is investigated. © 2000 American Vacuum Society.

[S0734-2101(00)04505-X]

## I. INTRODUCTION

The development of microtechnologies requires the optimization of the silicon-based materials derived from microelectronics for the realization of complex microelectromechanical systems (MEMS). As construction material or protective layer against alkaline solutions, silicon nitride  $\text{Si}_3\text{N}_4$  deposited by chemical vapor deposition (CVD) has not escaped this optimization.<sup>1–3</sup> In order to obtain higher deposition rate and lower tensile stress, the  $\text{SiH}_2\text{Cl}_2/\text{NH}_3$  gas mixture was replaced by the  $\text{SiH}_4/\text{NH}_3$  one. Further improvements in deposition rate and stress were achieved by depositing silicon rich silicon nitride  $\text{SiN}_x$  rather than stoichiometric silicon nitride  $\text{Si}_3\text{N}_4$ .<sup>4,5</sup> Finally, the formation of nitrogen doped silicon (NIDOS) film was briefly mentioned for the lowest  $\text{NH}_3/\text{SiH}_4$  gas ratio ( $R \approx 0.2$ ).<sup>5,6</sup>

In this article, we report the deposition and the characterization (optical, electrical, mechanical,...) of nitrogen doped silicon  $\text{SiN}_x$  films deposited by low-pressure chemical vapor deposition (LPCVD) from silane and ammonia for low  $\text{NH}_3/\text{SiH}_4$  gas ratio.

## II. EXPERIMENTS

NIDOS films were deposited by LPCVD from silane  $\text{SiH}_4$  and ammonia  $\text{NH}_3$  on 10 cm diameter, (111), oxidized (about 120 nm of oxide) silicon wafers (Fig. 1). Deposition runs were carried out at a temperature of  $750^\circ\text{C}$  (measured and controlled all along the 12-wafer load) and a total pressure  $P$  of 40.5 Pa. Silane flow was fixed at 100 sccm. Special atten-

tion was given to achieve low ammonia flows (from 0 to 20 sccm) and therefore low  $\text{NH}_3/\text{SiH}_4$  gas ratios  $R$  (from 0 to 0.2).

For each deposition experiment, the sixth and seventh wafers of a 12-wafer load were characterized. Films thickness and refractive index were assessed by ellipsometry at an 830 nm wavelength. Profilometry was used to check the ellipsometric results, to measure film roughness, and to determine films stress by wafer curvature measurements before and after removal of the rearside deposition by chemical etching in  $\text{HNO}_3$  ( $50\text{ cm}^3$ )/ $\text{CH}_3\text{COOH}$  ( $20\text{ cm}^3$ )/ $\text{HF}$  ( $1\text{ cm}^3$ ).<sup>5</sup> The influence of the nitrogen doping on film conductivity was assessed by four-probe measurements and film structure was analyzed by scanning electron microscopy (SEM) after dipping the samples into SECCO etch in order to make the polysilicon grains more distinct.

In addition, the deposited layers were studied by x-ray photoelectron spectroscopy (XPS) in order to characterize their composition  $\text{SiN}_x$ . XPS analyses were carried out with a Perkin Elmer PHI 5500 spectrometer with monochromatic Al  $K(\alpha)$ . For the experimental condition, the full width at half maximum of the Ag  $3d_{5/2}$  line was chosen at 1 eV. In order to get the N/Si ratio, Si  $2p$  and N  $1s$  photoelectron peaks were deconvoluted using a Shirley background subtraction method and a Gaussian–Lorentzian shape. The sample surface was sputtered with an  $\text{Ar}^+$  ion beam to eliminate the C and O adsorbed contamination layer.

## III. RESULTS AND DISCUSSION

### A. Deposition properties

In previous works, by applying the theory of heterogeneous media and the Bruggeman expression to the mix be-

<sup>a)</sup>Electronic mail: temple@laas.fr

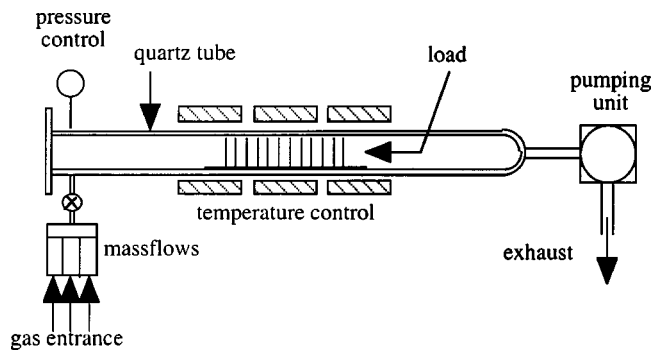


FIG. 1. Schematic representation of the LPCVD reactor.

tween polysilicon *p*-Si and stoichiometric silicon nitride Si<sub>3</sub>N<sub>4</sub>, a quasiparabolic relation between the refractive index  $n_{830\text{ nm}}$  and the N/Si ratio  $x$  has been derived from SiN<sub>*x*</sub> films<sup>5,6</sup>

$$n_{830\text{ nm}} = 3.7 - 1.83x + 0.42x^2. \quad (1)$$

Figure 2 represents the variations in the refractive index  $n_{830\text{ nm}}$  (measured by ellipsometry) as a function of the N/Si ratio (assessed by XPS spectroscopy) for the different deposited films. A good agreement is obtained between the Bruggeman theory and the experimental results. Since NIDOS has been defined as SiN<sub>*x*</sub> with  $x$  lower than 0.7, i.e., with refractive indexes  $n_{830\text{ nm}}$  higher than 2.625,<sup>5</sup> experimental results demonstrate that all the chosen deposition conditions have given nitrogen doped silicon rather than silicon rich silicon nitride films.

In order to understand the formation of nitrogen doped silicon and silicon rich silicon nitride, let us study the chemical system of the SiH<sub>4</sub>/NH<sub>3</sub> gas mixture by introducing the influences of radical species like silylene SiH<sub>2</sub>, monoaminosilane SiH<sub>3</sub>NH<sub>2</sub>, and silylamine SiH<sub>2</sub>NH<sub>2</sub>

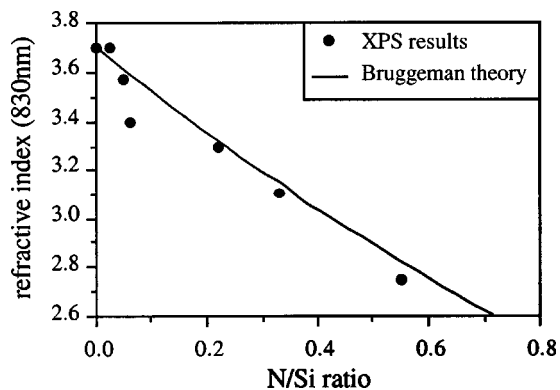
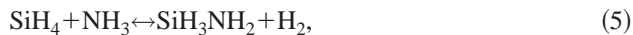
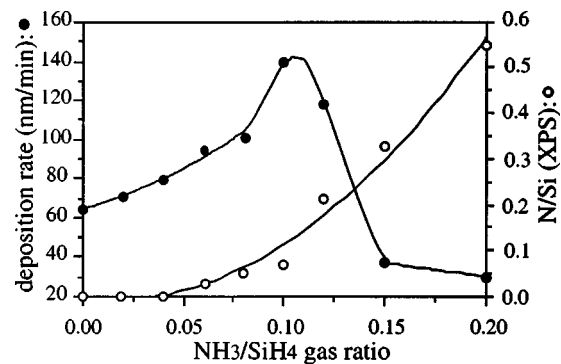
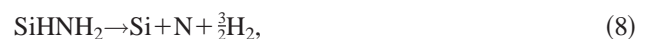
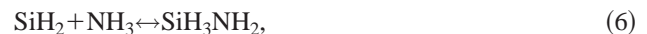
FIG. 2. Refractive index vs SiN<sub>*x*</sub> stoichiometry.

FIG. 3. Deposition rate and N/Si ratio vs gas ratio.



From these equations, it can be seen that each silane molecule leads to the deposition of a silicon atom into the film thanks to either the dissociative adsorption of SiH<sub>4</sub> [Eq. (3)] or SiH<sub>2</sub> [Eq. (4)] or SiH<sub>3</sub>NH<sub>2</sub> [Eq. (8)] species on the substrate. In the same way, each ammonia molecule leads to the deposition of a nitrogen atom into the film thanks to either the dissociative adsorption of SiH<sub>3</sub>NH<sub>2</sub> [Eq. (8)] or NH<sub>3</sub> [Eq. (9)] species on the substrate. Therefore, the N/Si ratio of the deposited films increases with the NH<sub>3</sub>/SiH<sub>4</sub> gas ratio as shown on Fig. 3.

The deposition rate variations with the NH<sub>3</sub>/SiH<sub>4</sub> gas ratio (also described on Fig. 3) are more complex. From a value ( $V_d \approx 64\text{ nm/min}$ ) obtained for pure silane ( $R=0$ ), the deposition rate increases with the gas ratio to reach a maximum of 140 nm/min for  $R=0.1$  and then decreases. This behavior can be explained by the SiH<sub>4</sub>/NH<sub>3</sub> chemical system given previously. For no ammonia flow, the silane pyrolysis is responsible for the formation of silylene SiH<sub>2</sub> [Eq. (2)] and silicon films are deposited thanks to both species [Eqs. (3) and (4)].

For low ammonia flow, NH<sub>3</sub> molecules react with both silane SiH<sub>4</sub> and silylene SiH<sub>2</sub> to form monoaminosilane SiH<sub>3</sub>NH<sub>2</sub> and silylamine SiH<sub>2</sub>NH<sub>2</sub> in the gas phase [Eqs. (5), (6), and (7)]. SiH<sub>4</sub>, SiH<sub>2</sub>, and SiH<sub>2</sub>NH<sub>2</sub> dissociate to deposit Si and N atoms [Eqs. (2), (3), and (8)] and nitrogen doped silicon films are deposited.

However, at higher flows, ammonia has opposite influences on the deposition kinetic. By reacting with silane SiH<sub>4</sub> [Eq. (3)] and by increasing the hydrogen H<sub>2</sub> concentration into the gas phase, it inhibits the silane pyrolysis [Eq. (2)] which leads to a decrease in the deposition rate.<sup>7</sup> By reacting with silylene SiH<sub>2</sub> [Eq. (4)], it is responsible for a shift of the silane pyrolysis equilibrium [Eq. (2)] towards the formation of more silylene and therefore for an increase in the deposi-

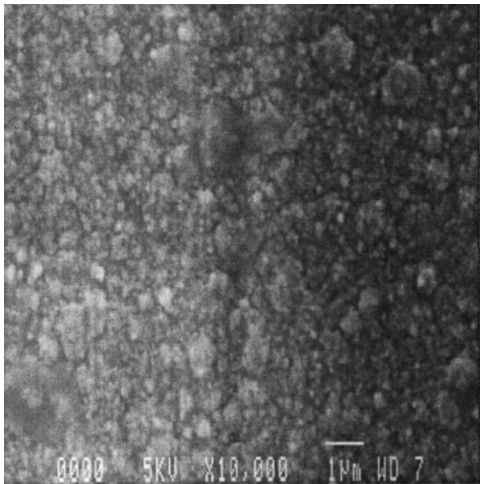


FIG. 4. Scanning electron micrograph of the  $R=0.1$  NIDOS film.

tion rate. As a consequence, the cumulative effects of these two phenomena explain the maximum in the deposition rate for a given gas ratio.

Finally, for high flow, ammonia controls completely the deposition mechanism. The inhibition of the silane pyrolysis [Eq. (2)] and the direct dissociation of  $\text{NH}_3$  [Eq. (9)] are responsible for the deposition of nitrogen atoms in excess and the formation of (silicon rich) silicon nitride films.

## B. NIDOS film properties

As a group-V atom, the nitrogen atom should act as a  $n$ -type substitutional impurity in silicon. In fact, it favors the insulative Si-N  $sp^2$ -like geometry rather than the conductive Si:N  $sp^3$ -like one.<sup>8</sup> As a result, this ambivalent phenomenon is responsible for a wide range of properties for the  $\text{SiN}_x$  films, going from (nitrogen doped) silicon to (silicon rich) silicon nitride. In the case of NIDOS films, this dual behavior is also responsible for competing mechanisms and therefore for complex variations of their different properties (structural, electrical, mechanical,...).

First, the NIDOS microstructure has been studied using SEM after dipping the samples into SECCO etch in order to make it more distinct. The NIDOS films deposited for  $R \leq 0.04$  are characterized by a typical polycrystalline structure while the heavily N doped NIDOS films deposited for  $R \geq 0.15$  are amorphous. Such behavior demonstrates that nitrogen doping into silicon films prevent them from crystallizing. More details on the polycrystalline/amorphous transition cannot be given: for gas ratio ranging from 0.06 to 0.12, the NIDOS films are characterized by a very rough surface with a lot of grains (Fig. 4) and SEM has not been successful in defining clearly their microstructure. NIDOS films roughness has therefore been studied as a function of the  $\text{NH}_3/\text{SiH}_4$  gas ratio  $R$ . Figure 5 shows that the mean roughness (measured by profilometry) follows similar variations as the deposition rate with a maximal value for  $R=0.1$ . This result suggests that roughness of NIDOS films should be related to deposition kinetic rather than to microstructure.

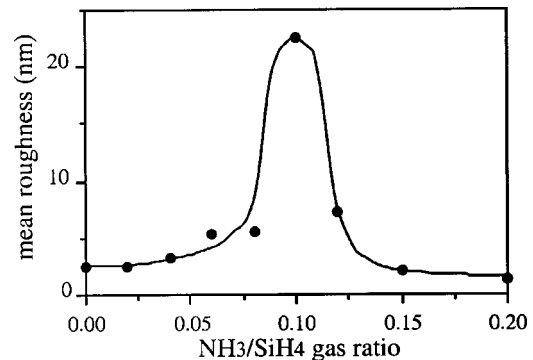


FIG. 5. Roughness vs gas ratio.

Then, electrical conductivity of NIDOS films has been studied by four-probe measurements. Figure 6 represents the variations of conductivity as a function of the  $\text{NH}_3/\text{SiH}_4$  gas ratio. Even if NIDOS is characterized by conductive properties, low conductivities are evidenced with a maximal value ( $\approx 95$  mS/cm) obtained for  $R=0.08$ . This maximum should be related to the dual influence of nitrogen atom into silicon (see later). The conductive Si:N  $sp^3$ -like geometry and the insulative Si-N  $sp^2$ -like one should be related respectively to the dissociative adsorption of  $\text{SiHNH}_2$  [Eq. (8)] and  $\text{NH}_3$  [Eq. (9)] species on the substrate. As a result and thanks to the proposed deposition mechanism (see Sec. III A), when the  $\text{NH}_3/\text{SiH}_4$  gas ratio  $R$  increases, i.e., when the N/Si ratio increases, fewer substitutional  $n$ -type impurities take part in the electrical conductivity increase and the insulative Si-N structure gradually takes over. The cumulative effects of these two phenomena explain the low electrical conductivity of the NIDOS films and the observed maximum in the conductivity for a given gas ratio. It should be noted that these maximal value obtained for  $R=0.08$  does not fit with the previous ones obtained for  $R=0.1$  (Figs. 2 and 5). No clear explanations for this misfit has been found up to now. It is assumed that the very rough structure obtained for  $R=0.1$  (Fig. 5) could be responsible for errors of the four-probe measurements technique, leading to the shift of the maximum towards lower gas ratio.

Finally, mechanical properties have been studied through residual stress-measurements, considering stress as an alge-

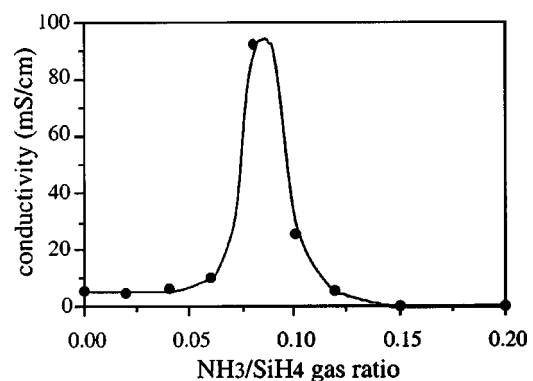


FIG. 6. Conductivity vs gas ratio.

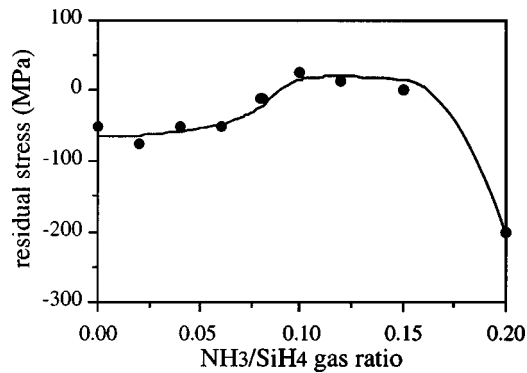


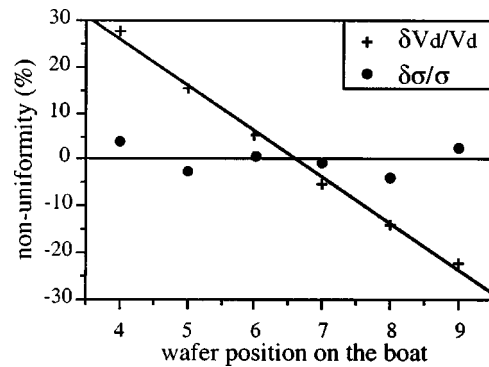
FIG. 7. Residual stress vs gas ratio.

braic value (a compressive stress is negative, a tensile stress positive). Figure 7 represents the variation in the NIDOS films residual stress as a function of the  $\text{NH}_3/\text{SiH}_4$  gas ratio  $R$ , showing a compressive/unstressed/compressive transition. Once again, the ammonia source, i.e., the nitrogen doping, has two opposite influences. The shrinkage of the film caused by the dissociation of Si-H and Si-N-H bonds and the rearrangement of the dangling bonds to form Si-Si and Si-N bonds are responsible for tensile stress.<sup>9</sup> Therefore, in the case of NIDOS deposition, the residual stress increases with the nitrogen doping, i.e., with the gas ratio. However, the gas ratio increase also prevents NIDOS film from crystallizing and is therefore responsible for a polycrystalline/amorphous transition (see later). Such transition has been related to a tensile/compressive one, i.e., to a stress decrease.<sup>10</sup> The cumulative effects of these two phenomena explain the maximum in the residual stress.

### C. Optimal deposition conditions for MEMS

The use of NIDOS can tackle many problems for the fabrication of MEMS. First, high deposition rates and therefore important film thickness, i.e., higher than  $1 \mu\text{m}$ , are easily obtained. Second, NIDOS optical properties are well known. Third, low stress or no stress NIDOS films are easily controlled. Of course, electrical properties are not excellent but can be further improved by conventional  $n$ -type or  $p$ -type doping.

In fact, the main drawback is related to the use of silane  $\text{SiH}_4$  which is responsible for consumption phenomena of the chemical species participating to the deposition and therefore for a decrease of the deposition rate along the load. These phenomena can be analyzed by studying the variations of deposition rate  $V_d$ , refractive index  $n$ , and residual stress  $\sigma$  along the load. Each wafer (from the fourth to the ninth) has been characterized by ellipsometry and profilometry and the different data obtained have been compared to the corresponding mean values (calculated on the sixth and seventh wafers) in order to study the relative variations of deposition rate  $\delta V_d/V_d$ , refractive index  $\delta n/n$  and/or residual stress  $\delta\sigma/\sigma$  (given in percent). Typical results obtained for silicon ( $R=0 - V_d \approx 64 \text{ nm/min} - n_{830 \text{ nm}} \approx 3.7 - \sigma \approx -50 \text{ MPa}$ ) and NIDOS ( $R=0.1 - V_d \approx 140 \text{ nm/min}$

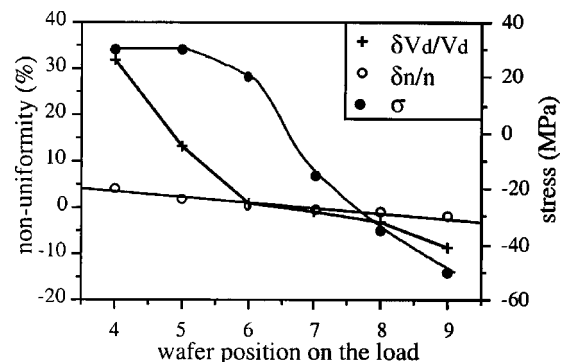
FIG. 8. Nonuniformity of deposition rate and residual stress along the load for the  $R=0$  silicon film.

$-n_{830 \text{ nm}} \approx 3.4 - \sigma \approx 0 \text{ MPa}$ ) depositions on a 12-wafer load are presented on Figs. 8 and 9, respectively. However, when the mean stress is quite nil,  $\delta\sigma/\sigma$  is more representative of measurements errors than consumption phenomena and the residual stress  $\sigma$  variations have been reported instead (Fig. 9).

At such high temperatures ( $\approx 750^\circ\text{C}$ ), and for silicon film deposition, consumption effects lead to thickness nonuniformity around  $\pm 30\%$  along the load. For NIDOS deposition and from the sixth wafer, nonuniformity of deposition rate and refractive index around  $\pm 10\%$  are obtained while film residual stress remains low ( $|\sigma| < 50 \text{ MPa}$ ). These results can be further improved by adding screen wafers in front of the useful load or by increasing the silane and ammonia flows. Such improvements will lead to an optimized deposition process of thick ( $1 \mu\text{m}$  and more), no-stress, (nitrogen doped) silicon films for MEMS fabrication.

### IV. CONCLUSION

An investigation of the LPCVD deposition of nitrogen doped silicon (NIDOS) films from  $\text{SiH}_4$  and ammonia  $\text{NH}_3$  has been done and the influences of the  $\text{NH}_3/\text{SiH}_4$  gaseous ratio on the different film properties have been studied. By changing the ammonia flow, varied nitrogen doping has been obtained in good agreement with the theory of heterogeneous media applied to the mix of polysilicon  $p$ -Si and silicon nitride  $\text{Si}_3\text{N}_4$ . Competing mechanisms of the  $\text{NH}_3/\text{SiH}_4$  gas

FIG. 9. Nonuniformity of deposition rate and refractive index and variations of residual stress along the load for the  $R=0.1$  NIDOS film.

ratio and maximal values have been evidenced for deposition rate, microstructure, electrical conductivity, and residual stress. They have been linked to the influence of radical species like silylene  $\text{SiH}_2$ , monoaminosilane  $\text{SiH}_3\text{NH}_2$ , and silylamine  $\text{SiH}_2\text{NH}_2$  into the gaseous phase, as well as to the dual behavior of the nitrogen atom into silicon.

Finally, optimal conditions have been found in order to deposit of thick, no-stress, NIDOS films for MEMS fabrication. They have already been already successfully used for the fabrication of microelectromechanical devices like micromotor or micropump.<sup>11</sup>

<sup>1</sup>M. Sekimoto, H. Yoshihara, and T. Ohkubo, *J. Vac. Sci. Technol.* **21**, 1017 (1982).

<sup>2</sup>J. G. E. Gardeniers, H. A. C. Tilmans, and C. C. G. Visser, *J. Vac. Sci. Technol. A* **14**, 2879 (1996).

<sup>3</sup>P. J. French, P. M. Sarro, R. Mollé, E. J. M. Fakkeldij, and R. F. Wolfenbuttel, *Sens. Actuators A* **58**, 149 (1997).

<sup>4</sup>K. E. Bean, P. S. Gleim, and R. L. Yeakley, *J. Electrochem. Soc.* **114**, 733 (1967).

<sup>5</sup>P. Temple-Boyer, C. Rossi, E. Saint-Etienne, and E. Scheid, *J. Vac. Sci. Technol. A* **16**, 2003 (1998).

<sup>6</sup>E. Dehan, P. Temple-Boyer, R. Henda, J. J. Pedroviejo, and E. Scheid, *Thin Solid Films* **266**, 14 (1995).

<sup>7</sup>E. Scheid, L. K. Kouassi, R. Henda, J. Samitier, and J. R. Morante, *Mater. Sci. Eng., B* **17**, 72 (1993).

<sup>8</sup>M. Saito and Y. Miyamoto, *Phys. Rev. B* **56**, 9193 (1997).

<sup>9</sup>A. G. Noskov, E. B. Gorokhov, G. A. Sokolova, E. M. Trukhanov, and S. I. Stenin, *Thin Solid Films* **162**, 129 (1988).

<sup>10</sup>P. Temple-Boyer, E. Scheid, G. Faugere, and B. Rousset, *Thin Solid Films* **310**, 234 (1997).

<sup>11</sup>M. Dilhan, J. Tasseli, D. Estève, P. Temple-Boyer, H. Camon, M. Anduze, and S. Colin, *Proceedings of SPIE: Design, Test and Microfabrication of MEMS and MOEMS* (1999), pp. 887–892.